Measurement of Electron Clouds in Large Accelerators by Microwave Dispersion

S. De Santis,[1] J. M. Byrd,[1] F. Caspers,[3] A. Krasnykh,[2] T. Kroyer,[3] M. T. F. Pivi,[2] and K. G. Sonnad[1]

[1]*Ernest Orlando Lawrence Berkeley National Laboratory, One Cyclotron Road, Berkeley, California 94720, USA*

[2]*Stanford Linear Accelerator Center, Menlo Park, California 94025, USA*

[3]*CERN, Geneva, Switzerland*

Clouds of low energy electrons in the vacuum beam pipes of accelerators of positively charged particle beams present a serious limitation for operation at high currents. Furthermore, it is difficult to probe their density over substantial lengths of the beam pipe. We have developed a novel technique to directly measure the electron cloud density via the phase shift induced in a TE wave transmitted over a section of the accelerator and used it to measure the average electron cloud density over a 50 m section in the positron ring of the PEP-II collider at the Stanford Linear Accelerator Center.

Low energy background electrons in the beam pipes of high energy accelerators of positively charged beams present a serious challenge to increasing current in these machines. Under the right machine conditions, such as bunch repetition rate, peak current, etc., amplification of the electrons can occur from secondary emission when the electrons strike the beam pipe walls, creating a growth in vacuum pressure along with a number of adverse effects on the circulating beam including severe two-stream instabilities, transverse beam blowup, and heating of cryogenic vacuum chambers. The net result is that the beam intensity is limited and beam quality reduced [1,2]. This effect is important for several future accelerators [3] such as the Large Hadron Collider (LHC) and the positron damping ring of the International Linear Collider (ILCDR), as well as several existing high intensity accelerators, such as the Accumulator Ring of the Spallation Neutron Source and the Tevatron Main Injector.

Electron cloud effects have been primarily observed in a number of high intensity synchrotrons and storage rings [4–13]. Experimental studies of the electrons have mainly used local detectors (retarding field analyzers) to measure the time dependence, density, and energy spectrum of the electron cloud in a small region near the detector [14–16]. However, the electron cloud density (ECD) can vary significantly along the beam pipe depending on local beam pipe geometry and surface conditions. Furthermore, the local measurement only detects those electrons that reach the beam pipe walls and can only infer the ECD with the help of computer simulation. Therefore, it is important to develop means of directly measuring the electron clouds over longer sections of the accelerator. Of course, one method of inferring the ring average ECD is from effects on the high energy beam itself, which usually only appear at relatively high beam intensities, however.

In this Letter, we present a novel idea [17] and its successful demonstration for measuring the ECD over a much longer section of a storage ring. This idea is based on measuring the time delay (i.e., phase shift) of a microwave signal propagating in the beam pipe due to the change of the index of refraction caused by the electron cloud. In practice, it would be challenging to measure the absolute phase shift of the signal, which is expected to be at most only a few degrees over a hundred meters, in an accelerator environment. Our idea relies instead on measuring the modulation of the phase shift of the microwave signal through the electron plasma by taking advantage of the modulation of the density of the electron cloud from gaps in the fill pattern of the circulating positive beam. If this gap is large enough, the electrons drift away and their density goes to zero, maximizing the modulation of the phase of the microwave signal. This technique differs from the local measurement of the ECD in several ways. The first is that our technique is a nondisruptive direct probe of the ECD in the beam pipe volume, regardless of the electron energy, over a much longer section of the accelerator. It also integrates primarily along the beam pipe axis, analogous to the effect of the plasma on the beam. The second difference is it does not require dedicated hardware and can be implemented anywhere in the ring between available electrodes.

A schematic of the measurement is shown in Fig. 1. It consists of a signal source which couples to an antenna on the beam pipe and excites the lowest frequency TE waveguide mode above the propagation cutoff frequency. The signal propagates through the beam pipe and electron plasma to another antenna and is analyzed on a receiver. The signal at the receiver has the form

$$s(t) = A\cos[\omega_{\mathrm{car}}t + \Delta\varphi(t)], \tag{1}$$

where $\Delta\varphi(t)$ is the time-dependent phase shift induced by the electron plasma and ω_{car} is the angular frequency of the transmitted signal. Because the repetition frequency of the high energy beam modulating the plasma density is the revolution frequency of the storage ring, we expect phase modulation sidebands of the main signal at multiples of the ring revolution frequency. The relative amplitude of these sidebands to the main signal allows us to determine the

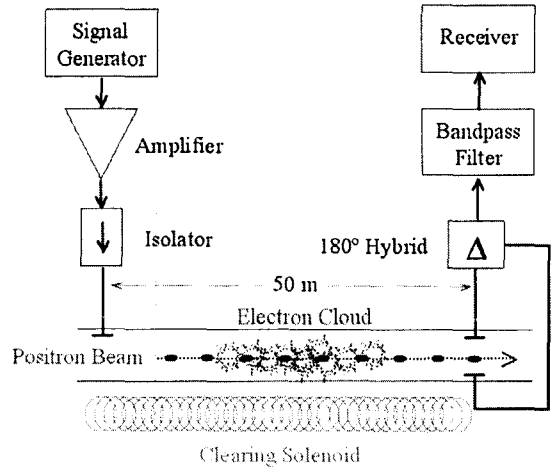

FIG. 1 (color online). Schematic diagram of experimental setup.

absolute value of the phase modulation, and thus the average ECD, and provides information about its time dependence. The primary experimental difficulty in making this measurement is the presence of the large beam induced signal at the receiver. This is discussed in detail later in this Letter.

The wave dispersion relation, which may be obtained by deriving the expression for the dielectric tensor, yields the value of $\Delta\varphi$. This has been studied in the past for plasma filled waveguides [18]. In the case of a beam pipe uniformly filled with an electron cloud and in the absence of an external magnetic field, the dispersion relation is [19]

$$k^2 = \frac{\omega^2}{c^2} - \frac{\omega_p^2}{c^2} - \frac{\omega_c^2}{c^2}, \tag{2}$$

where k is the wave number, c the speed of light, ω the wave frequency, ω_p the plasma frequency, and ω_c the beam pipe cutoff frequency. The plasma frequency ω_p is related to the electron density by $\omega_p \simeq 56.4\sqrt{n_e}$, where n_e is the electron density per cubic meter. Thus, the plasma frequencies for typical electron densities in beam pipes, of the order of $10^{12}\ e^-/\mathrm{m}^3$, are well below the beam pipe cutoff. The phase shift $\Delta\phi$ induced by the electron cloud over a propagation length L, in the limit of small plasma frequencies, can be obtained from Eq. (2) and is given by [20]

$$\Delta\varphi = \frac{L\omega_p^2}{2c(\omega^2 - \omega_c^2)^{1/2}}. \tag{3}$$

It is clear that the phase shift is proportional to the electron density and increases as the wave frequency approaches the pipe cutoff. Computation of the phase shift through particle-in-cell (PIC) simulations, using the plasma code VORPAL [21], under typical accelerator conditions shows good agreement with the above formula.

We performed the measurements in the low energy ring (LER) of the PEP-II B-Factory at the Stanford Linear Accelerator Center. The PEP-II LER has a typical positron beam current of 2.5 A with ~1700 bunches circulating in the 2.2 km circumference (136 kHz revolution frequency). For our measurements, the beam was uniformly distributed in bunches of 35–40 ps (rms) length, with a spacing of 4.2 ns and a gap of 100 ns (1.4% of the revolution period). At the typical beam current, assuming a chamber surface secondary electron yield of 1.4 in the LER stainless steel straight sections, an ECD of $1.2 \times 10^{12}\ e^-/\mathrm{m}^3$ is expected, giving a plasma frequency of 9.0 MHz and a phase shift of 1.1 mrad/m at a frequency of 2.15 GHz.

We transmitted the signal over a 50 m straight section of beam pipe in the LER in the IR12 region. The beam pipe is round with a diameter of 8.8 cm with a vacuum cutoff frequency of the lowest TE mode of 2 GHz. The antennas used to couple the microwave signal are two sets of button-type beam electrodes. A schematic of the measurement setup is shown in Fig. 1. An amplified signal generator excites the fundamental TE mode in the beam pipe, which propagates through the electron plasma and is detected by the spectrum analyzer acting as a very sensitive receiver. Note that the electrodes used are not optimized for coupling to the TE mode. For our experiment, assuming the ECD relaxes to zero during the gap in the beam, we expect a maximum phase modulation of 55 mrad. This yields a first order phase modulation sideband with an amplitude of 8×10^{-5} (−31 dB) with respect to the carrier signal.

The beam pipe in the IR12 region of the LER is wrapped with current carrying wires to generate a small solenoidal magnetic field [22]. This field is used to confine the electrons near the beam pipe walls, thus limiting their interaction with the positron beam and the emission of secondary electrons. In the region between our antennas there is a long solenoid, covering the entire distance, and six shorter solenoids. Each solenoid family generates a magnetic field of about 20 Gauss.

We chose a transmission (carrier) frequency of 2.15 GHz for several reasons. The first is to maximize the phase shift

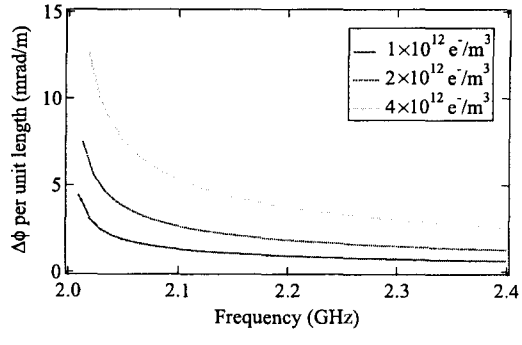

FIG. 2 (color online). Calculated phase shift per unit length for a uniform cold electron plasma in a waveguide with 2 GHz cutoff frequency.

from the ECD given by Eq. (2) while transmitting enough signal to observe the modulation. From Fig. 2, one sees that the phase shift increases for lower frequencies. However, signal attenuation also increases and we found an optimum near 2.15 GHz. The second reason for the frequency choice is to avoid frequencies in the spectrum of the much stronger beam signal. For the LER beam, the primary signals occur at harmonic frequencies of the bunch repetition rate of 238 MHz, with intermediate signals at multiples of the ring revolution frequency of 136 kHz. Furthermore, the beam can also oscillate at synchrotron and betatron frequencies with signals that can appear in between the signals at the revolution frequency harmonics. Therefore, we chose our frequency to clearly avoid these frequencies. The third reason is that this frequency is well below the cutoff frequency of the next propagating beam pipe mode.

An example of a measurement of the electron-cloud-induced phase shift is shown in Fig. 3. The first plot shows the power spectrum of the receiver signal with the solenoid field at 40 G. The carrier signal is evident as well as two beam revolution harmonic signals with small synchrotron oscillations sidebands. When the solenoid field is set to zero, the beam pipe fills with electrons and a sideband of the transmission carrier is observed. Assuming that the phase modulation is purely sinusoidal and that the ECD reaches zero during the gap, this modulation indicates an average electron density of $6.6 \times 10^{11}\ e^{-}/\mathrm{m}^3$. This effect is reproducible.

With the large beam signals present at both electrodes, it is possible that modulation sidebands of the transmitted carrier appear from intermodulation with the beam signal at either the receiver or transmitter. We took several steps to minimize this possibility. To reduce the amplitude of the beam induced signal, we used the difference signal from two opposing beam electrodes, combined in a 180° hybrid.

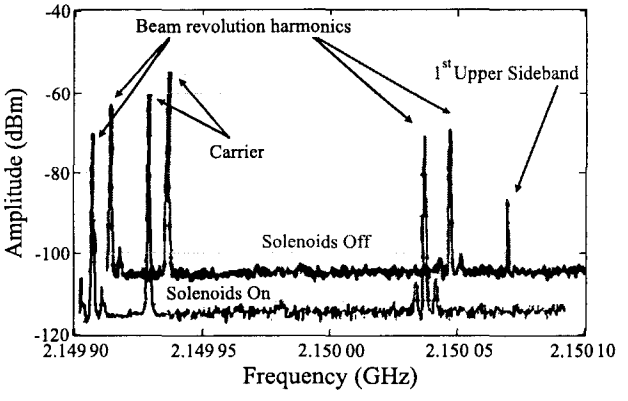

FIG. 3 (color online). Spectrum analyzer traces showing microwave carrier and beam signals. A phase modulation sideband appears when the solenoid field is turned off, allowing the electron plasma to fill the beam pipe. Only the upper sideband is shown.

Furthermore, we used a bandpass filter centered at 2.15 GHz with a bandwidth 540 MHz which reduced the total power of the beam signal by at least 15 dB. We also verified that the measured phase modulation did not depend on the amplitude of the carrier signal. We inserted an isolator between the amplifier and antenna to avoid intermodulation at the transmitter from the beam signal pickup on the transmission electrodes. With no beam, only the carrier signal is present. Modulation sidebands appear above the noise floor of the spectrum analyzer above a beam current of 1.7 A. Improved signal transmission would increase the sensitivity of the phase modulation detection at lower beam currents.

The above estimate using the first modulation sideband only yields an average value of the ECD. Ideally, the time dependence of the ECD can be obtained by directly demodulating the transmitted carrier signal. The presence of large beam signals makes this difficult and direct demodulation of the phase shift would require more sophisticated filtering techniques. Because the bandwidth of the modulation measured in the frequency domain is inversely related to the rise and fall time of the phase modulation [23] $\Delta\varphi(t)$, it is possible to estimate the growth and decay time of the electron cloud by measuring the distribution of the modulation sidebands. Shown in Fig. 4 is the measured amplitude of modulation sidebands relative to the carrier signal. If we assume that the ECD grows at the start of the positron bunch train and decays during the gap in the bunch train, we can estimate the rise time to be no more than one seventh of a revolution period, or 1.0 ms.

As an example of the utility of this technique, we characterized the effectiveness of the solenoid field in controlling the ECD over the IR12 straight section. Shown in Fig. 5 is an estimate of the average ECD derived from the first modulation sideband as a function of the solenoid strength. This measurement indicates that only small solenoid fields are required to confine the electron cloud near the beam pipe walls and limit the ECD.

In summary, we have demonstrated a novel method for measuring the density of electron clouds in a positron

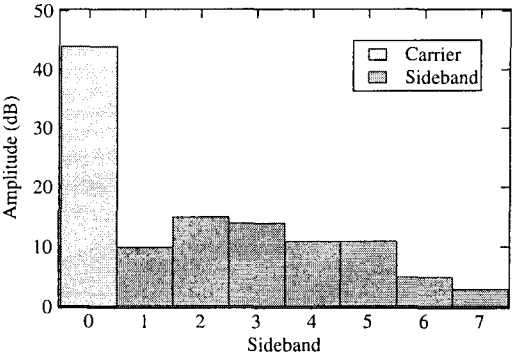

FIG. 4 (color online). Harmonics of the phase modulation sidebands extracted from spectrum analysis.

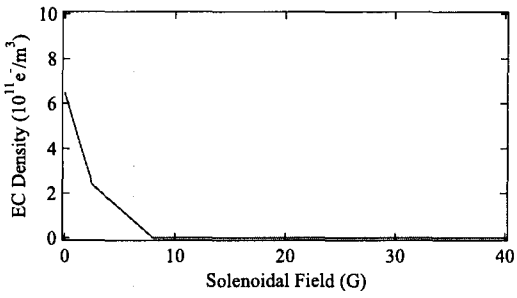

FIG. 5 (color online). Average electron cloud density derived from the first modulation harmonic as a function of the beam pipe solenoid field.

storage ring over a relatively long section of the accelerator beam pipe. This technique is ideal for this application because it provides an independent means of identifying the electron cloud presence and density in a regime where it presents a limitation to the accelerator performance. It also complements present local measurement techniques in that it directly probes the ECD in the beam pipe volume. It may be the only present means of characterizing the overall effectiveness of EC mitigation techniques such as solenoid fields, vacuum chamber coatings and geometries, and clearing electrodes.

The authors wish to thank R. Akre, U. Wienands, A. Fisher, M. Sullivan, F.-J. Decker, S. Hoobler, W. Wittmer, Z. Van Hoover, and A. Kulikov for their help with the experiments, and M. Furman for useful discussions. Work supported by the Director, Office of Science, Office of High Energy Physics and Basic Energy Sciences, of the U.S. Department of Energy under Contracts No. DE-AC02-05CH11231, No. DE-AC03-76SF00515, and No. DE-AC02-07CH11359.

[1] K. Ohmi, Phys. Rev. Lett. **75**, 1526 (1995).
[2] K. Ohmi and F. Zimmermann, Phys. Rev. Lett. **85**, 3821 (2000).
[3] R. Cimino, I. R. Collins, M. A. Furman, M. Pivi, F. Ruggiero, G. Rumolo, and F. Zimmermann, Phys. Rev. Lett. **93**, 014801 (2004).
[4] M. Izawa, Y. Sato, and T. Toyomasu, Phys. Rev. Lett. **74**, 5044 (1995).
[5] O. Grobner, in *Proceedings of the Xth International Conference on High Energy Accelerators, Serpukhov, 1977* (USSR Academy of Sciences, Moscow, 1977), Vol. 2, pp. 277–282.
[6] D. Neuffer *et al.*, Nucl. Instrum. Methods Phys. Res., Sect. A **321**, 1 (1992).
[7] M. Tobiyama, J. W. Flanagan, H. Fukuma, S. Kurokawa, K. Ohmi, and S. S. Win, Phys. Rev. ST Accel. Beams **9**, 012801 (2006).
[8] G. Arduini, K. Cornelis, W. Hofle, G. Rumolo, and F. Zimmermann, in *Proceedings of the 2003 Particle Accelerator Conference, Portland, Oregon* (IEEE, Piscataway, NJ, 2003).
[9] K. C. Harkay and R. A. Rosenberg, Phys. Rev. ST Accel. Beams **6**, 034402 (2003).
[10] D. Schulte, G. Arduini, V. Baglin, J. M. Jiménez, F. Ruggiero, and F. Zimmermann, in *Proceedings of the 2005 Particle Accelerator Conference, Knoxville* (LHC Project Report 847, 2005).
[11] A. Kulikov, A. Fisher, S. Heifets, J. Seeman, M. Sullivan, U. Wienands, and W. Kozanecki, in *Proceedings of the 2001 Particle Accelerator Conference, Chicago* (IEEE, Piscataway, NJ, 2001), pp. 1903–1905.
[12] Q. Qin, ZY. Guo, H. Huang, Y. D. Liu, J. Xing, J. Q. Wang, and Z. Zhao, Nucl. Instrum. Methods Phys. Res., Sect. A **547**, 239 (2005).
[13] W. Fischer, J. M. Brennan, M. Blaskiewicz, and T. Satogata, Phys. Rev. ST Accel. Beams **5**, 124401 (2002).
[14] R. A. Rosenberg and K. C. Harkay, Nucl. Instrum. Methods Phys. Res., Sect. A **453**, 507 (2000).
[15] K. I. Kanazawa, H. Fukuma, H. Hisamatsu, and Y. Suetsugu, in *Proceedings of the 2005 Particle Accelerator Conference, Knoxville* (IEEE, Piscataway, NJ, 2005), p. 1054.
[16] M. Kireeff Covo *et al.*, Phys. Rev. Lett. **97**, 054801 (2006).
[17] F. Caspers, W. Höfle, J. M. Jiménez, J. F. Malo, J. Tuckmantel, and T. Kroyer, in *Proceedings of the 31st ICFA Beam Dynamics Workshop: Electron Cloud Effects (ECLOUD04), Napa, California 2004* (CERN Report No. CERN-2005-001, 2004).
[18] A. W. Trivelpiece and R. W. Gould, J. Appl. Phys. **30**, 1784 (1959).
[19] H. S. Uhm, K. T. Nguyen, R. F. Schneider, and J. R. Smith, J. Appl. Phys. **64**, 1108 (1988).
[20] K. Sonnad, M. Furman, S. Veitzer, P. Stoltz, and J. R. Cary, in *Proceedings of the 2007 Particle Accelerator Conference, Albuquerque, New Mexico, 2007* (IEEE, Piscataway, NJ, 2007).
[21] C. Nieter and J. R. Cary, J. Comput. Phys. **196-2**, 448 (2004).
[22] A. Kulikov, A. Novokhatski, and J. Seeman, in *Proceedings of the 31st ICFA Beam Dynamics Workshop: Electron Cloud Effects (ECLOUD04), Napa, California, 2004* (SLAC Report No. SLAC-PUB-10886, 2004).
[23] J. R. Carson, Proc. IRE, **10**, 57 (1922).